Electronic and thermoelectric properties of $AgBi_3Se_5$ and $AgBi_3S_5$ materials: A first-principles study

T Santillán-Gómez, F Puch, and J. C. Martínez-Orozco

Unidad Académica de Física, Universidad Autónoma de Zacatecas, Av. solaridad, Zacatecas, 98068, Zacatecas, México.

Received 7 April 2025; accepted 14 July 2025

In this work, the structural, electronic and thermoelectric properties were calculated for the thermoelectric materials $AgBi_3S_5$ and $AgBi_3Se_5$ using Density Functional Theory (DFT). The aim was to determine the total density of states and the partial density of states, the Seebeck coefficient, electrical conductivity, thermal conductivity, and merit factor of both systems. The electronic properties are studied using the modified Becke-Johnson Tran-Blaha (TB-mBJ) potential (2009) for the exchange-correlation potential. The study of the electronic properties shows that the total density of states of $AgBi_3S_5$ and $AgBi_3Se_5$ are similar, close to the Fermi energy, and in general, they are similar, only presenting some higher peaks below the Fermi energy. This is due to the partial density of states of the Se atoms. The Seebeck coefficient, electrical conductivity, thermal conductivity, and figure of merit of $AgBi_3S_5$ correspond with the experimental results. While $AgBi_3Se_5$ presents better figure of merit values in the temperature range from 500 to 800 K, in this temperature range this material presents a better Seebeck coefficient. The highest value for figure of merit was 0.441 for $AgBi_3Se_5$ at a temperature of 800 K.

Keywords: Density functional theory; thermoelectric properties; figure of merit.

DOI: https://doi.org/10.31349/RevMexFis.72.011001

1. Introduction

The energy crisis remains a problem today. Thermoelectricity offers an alternative in energy recovery, as it converts heat into electricity without any moving parts but through the use of thermoelectric materials [1,2]. The study of these materials has recently garnered interest since they have environmental benefits and different applications not only in heat recovery but also in cooling systems, as well as in outer space where spacecraft are made of thermoelectric materials of high temperature (>975 K)[3,4]. The efficiency of thermoelectric materials can be measured by the thermoelectric figure of merit of dimensionless quantities such as:

$$zT = \frac{S^2\sigma}{\kappa}T, \tag{1}$$

where S, σ, κ and T represent the Seebeck coefficient, electrical conductivity, thermal conductivity, and absolute temperature, respectively. The Seebeck coefficient of a material measures the amount of voltage induced by a temperature difference. Electrical conductivity per relaxation time (σ/τ) allows us to understand the connection between current and free carriers (electrons/holes). The power factor (PF) is defined as $PF = S^2\sigma$; this quantity allows measuring the potential of any thermoelectric material, and determines the ability of a material to produce electrical energy at a given temperature. Thermal conductivity depends on the vibrations of the crystal lattice and the electrons, $k = k_e + k_l$ indicates that lattice vibrations are responsible for heat conduction, while thermal conductivity in metals is caused by free electrons [5,6]. To obtain better thermoelectric performance in a composite, low thermal conductivity per relaxation time (κ/τ) is required [7]. These properties can be calculated using the Boltzmann-Madsen theory [9], where for example the Seebeck coefficient is found in terms of the moments of the generalized transport coefficients ($\mathcal{L}^\alpha$):

$$S = \frac{1}{qT}\frac{\mathcal{L}^1}{\mathcal{L}^0}. \tag{2}$$

Currently, there are some materials with zT close to unity near room temperature [9]. More materials with values close to unity are necessary, as this would allow for technological application since the industry demands materials with higher zT values. Independent optimization of all these quantities of thermoelectric transport is not easy. However, through the study of structural and alloy engineering, it is possible to optimize these parameters [10,11]. This opens the door to both theoretical and experimental studies to carry out these optimizations. At the same time, some software has been developed to help determine the figure of merit and thus select the most promising materials [12]. One of these software is the case of the BoltzTraP2 [8] code which uses semi classical Boltzmann-Madsen transport theory and has been used efficiently in the calculation of thermoelectric properties of $YbMg_2X_2$ (X = P, As, Sb, Bi) Zintl Compounds [13].

Another material that promises to be a good thermoelectric is the $AgBi_3S_5$ compound. Due to its low thermal conductivity and its environmentally compatible composition. At room temperature, the electrical conductivity is 489 S/cm, with a thermoelectric power of -64 μV/K. The thermoelectric conductivity is very low, approximately 1 W/mK [14]. The compounds $Bi_{2-x}Ag_{3x}S_3$ ($x = 0-0.06$) were manufactured using mechanical alloying (MA) and spark plasma sintering (SPS). For different doping concentrations, the maximum value of zT is 0.23 and is reached at 573 K for

the $Bi_{1.99}Ag_{0.03}S_3$ sample, which is 130% higher than that (0.11) of the pure Bi_2S_3 [15]. By increasing the temperature from 323 K to 573 K, the Seebeck coefficient of $AgBi_3S_5$ varies from -83 μV/K to -167 μV/K, while the electrical conductivity of $AgBi_3S_5$ decreases from 178 S/cm to 79 S/cm, thereby a maximum power factor 221 $\mu Wm^{-1}K^{-2}$ is achieved at 573 K. It is notable that the $AgBi_3S_5$ has a low thermal conductivity, ranging from 0.70 to 0.64 Wm^{-1} K^{-1} from 323 K to 573 K, and then a peak thermoelectric figure of merit value of 0.20 is obtained at 573 K [16]. G. Tan *et al.* used the element Cl to dope $AgBi_3S_5$, thereby obtaining low thermal conductivities of $0.5-0.3$ $Wm^{-1}K^{-1}$ in the temperature range of 300 K-800 K. When the doping concentration is 0.33%, the figure of merit reaches 1.0 in 800 K [17].

Recently, Wu *et al.* [18] combined carrier concentration modulation and entropy engineering techniques, employing melt-annealing and spark plasma sintering, to synthesize a series of $AgBi_3(Se_{5y}S_{1-y})_{5.08}$ bulk materials. Their results showed that doping the $AgBi_3S_5$ compound with Se atoms reduces thermal conductivity, thereby enhancing the thermoelectric figure of merit (zT). This suggests that $AgBi_3Se_5$ could be a promising candidate with superior thermoelectric performance.

Among existing theoretical studies, the work by Guo *et al.* [19] stands out as one of the most relevant contributions, providing a detailed analysis of the thermoelectric properties of $AgBi_3S_5$ using first-principles calculations and Boltzmann transport theory. In their methodology, the authors employed the pseudopotential approach within the framework of the generalized gradient approximation (GGA) using the Perdew-Burke-Ernzerhof (PBE) functional, along with the constant relaxation time approximation (CRTA). To improve the accuracy of band structure calculations, they also used the Tran-Blaha modified Becke-Johnson (TB-mBJ) potential. Furthermore, they modeled different doping levels by shifting the Fermi level and analyzed the anisotropy of electronic and transport properties along various crystallographic directions. Their results for the Seebeck coefficient, electrical conductivity, power factor, and zT showed good agreement with experimental data, providing a solid theoretical foundation for the computational study of this family of materials.

However, despite the value of these studies, the theoretical understanding of the $AgBi_3Se_5$ compound remains limited. The present work aims to expand upon the framework established by Guo and other researchers by performing a first-principles comparative analysis between $AgBi_3S_5$ and $AgBi_3Se_5$, in order to understand how substituting sulfur with selenium affects the electronic structure and thermoelectric properties. This approach provides new insights into the behavior of these compounds within a consistent theoretical framework.

2. Computational method

All computations were performed using the WIEN2K code 2009 [20], which is based on density functional theory (DFT) and employs a full potential (FP). The code uses a base of Linearized Augmented Plane Wave to which local orbitals are added (LAPW+lo). The modified Becke-Johnson Tran-Blaha (TB-mBJ) potential of 2009 [21] was used for the exchange-correlation potential, which can reproduce accurate bandgap of semiconductors. The separation energy between the nucleus and valence states was set at 6.0 Ry. The number of k points used to make the sampling in the first Brillouin zone is 1000. The radius *muffin tin* was set equal to 2.5, 2.46, 2.08, and 2.5 for the Ag, Se, S and Bi atoms, respectively. In addition to the convergence in energy (0.0001 Ry). Similarly, thermoelectric properties were assessed by semi-classical Boltzmann transport theory [22] implemented in BoltzTrap2 code [8]. This code has already been used successfully in the calculation of thermoelectric properties. Such is the case of the studies carried out by [13] where he studied thermoelectric properties of $YbMg_2X_2$ (X = P, As, Sb, Bi) zintl compounds.

3. Results and discussions

The crystal structure of $AgBi_3S_5$ and $AgBi_3Se_5$ is shown in Fig. 1. Both compounds have a monoclinic structure and belong to the C2/m space group. $AgBi_3S_5$ optimized crystal lattice parameters are $a = 13.57$ Å, $b = 4.06$ Å, and $c = 16.56$ Å, $\alpha = \gamma = 90°$, and $\beta = 95.17°$ [14], and $AgBi_3Se_5$ optimized crystal lattice parameters are $a = 14.046$ Å, $b = 4.192$ Å, and $c = 17.318$ Å, $\alpha = \gamma = 90°$, and $\beta = 95.581°$ [23]. The relative positions for the Ag, Bi, Se, and S atoms in the monoclinic structure are shown in Table I.

Band structure

The band structures for $AgBi_3S_5$ and $AgBi_3Se_5$ are shown in Fig. 2a) and 2b), respectively. The band structure of $AgBi_3S_5$

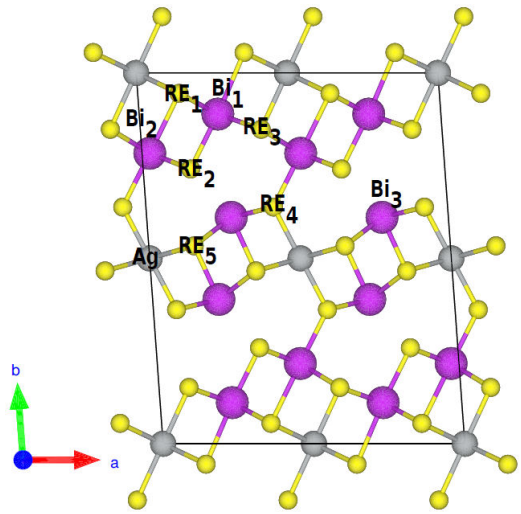

FIGURE 1. Crystalline structure C2/m of $AgBi_3S_5$ and $AgBi_3Se_5$. Here, the positions indicated in this figure correspond to those highlighted in bold in Table I.

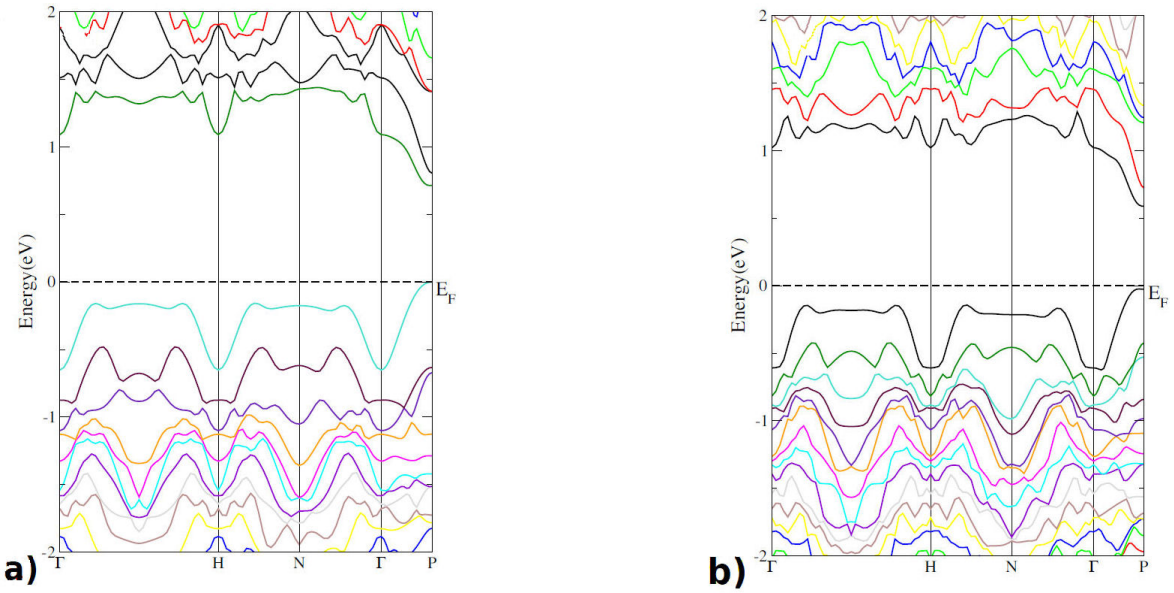

FIGURE 2. Electronic band structure of (a) $AgBi_3S_5$ and (b) $AgBi_3Se_5$.

TABLE I. Relative positions for the atoms of the compounds $(AgBi_3Re_5)_2$ where Re= Se or S. The positions in bold correspond to the atoms marked in Fig. 1.

Atom	*a*	*b*	*c*
Ag	0.0	0.0	0.0
	0.0	**0.5**	**0.5**
Bi	0.739	0.111	0.0
	0.261	**0.889**	**0.0**
	0.974	0.217	0.5
	0.026	**0.783**	**0.5**
	0.219	0.389	0.0
	0.780	**0.611**	**0.0**
Re	0.862	0.055	0.5
	0.138	**0.945**	**0.5**
	0.843	0.259	0.0
	0.157	**0.741**	**0.0**
	0.599	0.152	0.5
	0.401	**0.848**	**0.5**
	0.077	0.362	0.5
	0.423	**0.638**	**0.5**
	0.849	0.466	0.0
	0.150	0.**534**	**0.0**

$AgBi_3S_5$ corresponds to that reported in the literature [14] where we used the generalized gradient approximation (GGA) of Perdew, Burke, and Ernzerhof for the exchange-correlation potential [24]. Both band structures have the behavior of semiconductor materials, with the difference that for the $AgBi_3Se_5$, the energy bandgap is 0.272 eV, which is lower than that of $AgBi_3S_5$, which is of 0.435 eV. The bandgap of $AgBi_3Se_5$ is 37.5 % smaller than the one of $AgBi_3S_5$. In the range of -2 to 2 eV, $AgBi_3Se_5$ contains a higher number of electronic bands, which makes it a better thermoelectric material and could present better values in the figure of merit.

Density of states

The total density of states (TDOS) are shown in Fig. 3a). The TDOS of $AgBi_3S_5$ corresponds to that reported in the literature by Kim [14] and Guo [19] where they worked with the Perdew-Burke and Ernzerhof [24] and TB-mBJ [21] approximations, respectively. In this work, the LAPW+lo method was used. The potential TB-mBJ was also used because this one presents better results in this type of materials. In the region close to Fermi energy, the TDOS of $AgBi_3Se_5$ and $AgBi_3S_5$ are similar. The only difference is that the TDOS of $AgBi_3Se_5$ is slightly higher. Figures 3b) and 3c) show the partial density of states (PDOS) for the S and Se atoms of the $AgBi_3S_5$ and $AgBi_3Se_5$ materials, respectively. The contributions to the TDOS of these atoms are similar. It is important to note that for the TDOS, at the energy -0.19 eV, there exists a local maximum for both materials. This maximum comes from the contributions of the atoms located in positions RE4 and RE5 in Figs. 3b) and 3c). These contributions play an important role in thermoelectric properties. For the next maximum below of this value, the contributions come from atoms located in positions RE1, RE2 and RE3.

Transport properties

To calculate electrical conductivity, Seebeck coefficient and thermal conductivity in terms of temperature, the code BoltzTraP2 is used. This code uses the semi-classical transport theory [25] and the electronic properties previously calculated for these materials. The calculated Seebeck coefficient as a

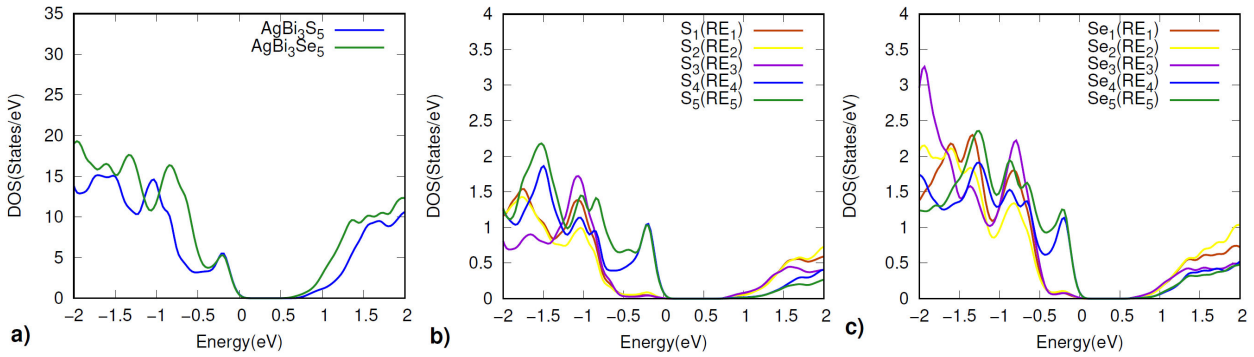

FIGURE 3. a) TDOS of $AgBi_3S_5$ and $AgBi_3Se_5$. PDOS for the S of b) $AgBi_3S_5$, and for the Se of c) $AgBi_3Se_5$. Here, the S_i are the sulfur atoms of $AgBi_3S_5$ and the Se_i are the selenium atoms of $AgBi_3Se_5$.

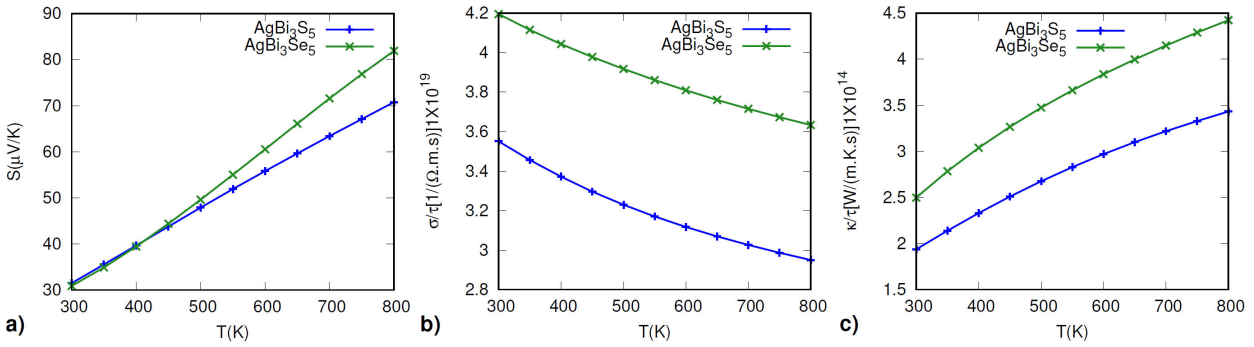

FIGURE 4. The calculated a) Seebeck coefficient, b) Electrical conductivity and c) Thermal conductivity.

function of temperature is shown in Fig. 4a). Both materials show positive Seebeck coefficient values for the full temperature regime (300 to 800 K). This may indicate p-type behavior [26]. However, experimental results reveal that the material exhibits n-type behavior. This discrepancy in the sign of the Seebeck coefficient can be attributed to the presence of silver atoms, which are among the few elements (along with Cu, Ag, Au, and Li) for which the sign of the Seebeck coefficient (S) is opposite to that of the dominant charge carriers [27]. Within the framework of Boltzmann transport theory, as formulated by Allen, the predicted sign of S necessarily corresponds to that of the charge carriers. At room temperature 300K, the Seebeck coefficient value of $AgBi_3S_5$ is 31.5 $\mu V/K$ and for $AgBi_3Se_5$ is 30.9 $\mu V/K$. However, for temperatures higher than 450 K the values of $AgBi_3Se_5$ are higher than those of $AgBi_3S_5$. The experimental results reported by Y. Wu *et al.* [18] indicate that the Seebeck coefficient values of $AgBi_3Se_5$ are approximately twice those of $AgBi_3S_5$. However, in the present study, our results show similar values for both compounds, although they qualitatively reproduce the expected behavior. These results could potentially be improved by considering electron-phonon coupling in the calculations

Figure 4b) shows the graph of variational electrical conductivity per relaxation time vs. temperature. The graph shows the linear variational behavior of both materials with temperature. At room temperature, the electrical conductivity value of $AgBi_3S_5$ is 3.6×10^{19} Ω^{-1} $m^{-1}s^{-1}$, and for $AgBi_3Se_5$ it is 4.2×10^{19} Ω^{-1} $m^{-1}s^{-1}$. These materials have relatively higher electrical conductivity than conventional thermoelectric materials, which reduce the Joule heating effect [28] and suggests they may be supposed to be good thermoelectric materials. Figure 4c) shows a graph of thermal conductivity vs. temperature for the compounds $AgBi_3S_5$ and $AgBi_3Se_5$. For both materials the thermal conductivity per relaxation time (κ/τ) has its lowest values at room temperature 300 K, which are 1.94×10^{14} W/m.K^2.s for $AgBi_3S_5$ and 2.5×10^{14} W/m.K^2.s for $AgBi_3Se_5$. In the graph, you can be observed an increase in the power factor as the temperature increases, which is a characteristic of a good thermoelectric material. The values of the figure of merit are those reported in the literature, as they facilitate comparison with other materials. In the Boltzmann-Madsen theory [8], used to describe transport properties in solids, the electrical conductivity (σ) and the electronic thermal conductivity (κ_e) are calculated within the constant relaxation time approximation. BoltzTraP2 assumes that the τ is constant and independent of energy, temperature, and momentum. Therefore, transport properties such as σ and κ_e are reported in a form proportional to τ, that is, as σ/τ and κ_e/τ. When calculating the thermoelectric figure of merit $zT = S^2\sigma T/\kappa_e + \kappa_l$, if only the electronic contribution considered and the expressions of σ and κ_e obtained from this theory are used, the parameter τ cancels out. This allows for a qualitative comparison of

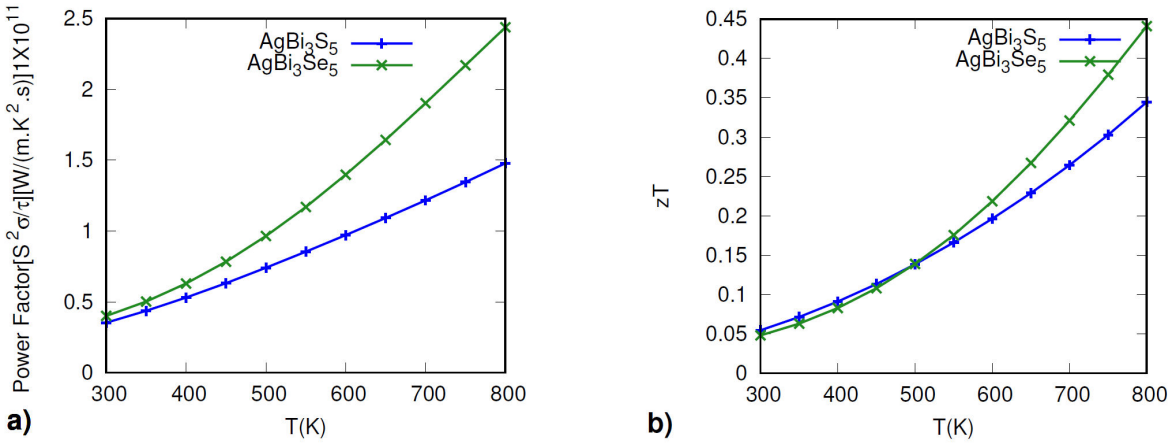

FIGURE 5. a) Power factor and b) Figure of merit (zT) vs temperature of $AgBi_3S_5$ and $AgBi_3Se_5$.

thermoelectric performance without requiring the exact value of τ.

After obtaining the transport parameters in terms of temperature, it is possible to calculate the power factor (PF) and the figure of merit (zT) of compounds $AgBi_3S_5$ and $AgBi_3Se_5$ in terms of temperature. Figure 5a) shows the power factor vs temperature for $AgBi_3S_5$ and $AgBi_3Se_5$. The room temperature value of PF for $AgBi_3S_5$ and $AgBi_3Se_5$ is 3.5×10^{10} W/mK^2.s and 4×10^{10} W/m.K^2.s, respectively. Figure 5b) shows the graph of zT as a function of temperature for both compounds in the temperature range ($300 - 800$ K). It is observed that the zT of $AgBi_3S_5$ and $AgBi_3Se_5$ intersect at approximately 500 K. These results qualitatively agree with previously reported studies on $AgBi_3S_5$. At room temperature, the zT value of $AgBi_3S_5$ is 0.054, and that of $AgBi_3Se_5$ is 0.048. In the temperature range of 500-800 K $AgBi_3Se_5$ presents better values in zT, this seems to be due to the fact that in this region it presents better values of the Seebeck coefficient than $AgBi_3S_5$. The highest value for zT was 0.441 for $AgBi_3Se_5$ at a temperature of 800 K. As in the studies conducted by G. Tan *et al.* [17], substituting S atoms with Se in $AgBi_3S_5$ significantly improves the thermoelectric and electronic properties at 800 K. This improvement is partly due to a reduction in the bandgap when replacing S with Se, which increases the electrical conductivity. Consequently, $AgBi_3Se_5$ stands out as a promising material for future investigations. One possible research direction would be to explore doped systems of this compound with Cl, S, or other elements that could further improve its thermoelectric performance.

4. Conclusion

In this work, the total and partial density of states, the band structure, and the thermoelectric properties of $AgBi_3S_5$ and $AgBi_3Se_5$ were determined. The TDOS and PDOS of $AgBi_3S_5$ are consistent with previous studies. The $AgBi_3S_5$ and $AgBi_3Se_5$ exhibit the characteristics of semiconductor materials, with $AgBi_3Se_5$ having the smallest band gap of 0.272 eV. Because the PDOS of the Se atoms is very similar to that of the S atoms, the TDOS of $AgBi_3S_5$ and $AgBi_3Se_5$ are also quite similar near the Fermi energy, with the TDOS of $AgBi_3Se_5$ being slightly higher. The PDOS of atoms at the Re_4 and Re_5 positions plays a significant role in the TDOS near the Fermi energy. The results show that $AgBi_3Se_5$ has a higher electrical conductivity, thermal conductivity, and power factor within the temperature range of 300-800 K compared to $AgBi_3S_5$. It is important to emphasize that the focus here is on the qualitative behavior of these properties, rather than on precise quantitative values. This qualitative agreement aligns with previously reported studies and supports the observed trends in thermoelectric performance. As well as a higher merit figure (zT) in the range of 500-800 K, while $AgBi_3S_5$ shows a better zT in the range of 300-500 K. This latest result is consistent with the experimental findings [18] (for $AgBi_3(Se_{0.9}S_{0.1})_{5.08}$, $AgBi_3S_{5.08}$, $AgBi_3Se_5$, $AgBi_3S_5$ respectively), except at the temperature where they change (approximately at 450 K). Finally, experimental results show that the Seebeck coefficient of $AgBi_3S_5$ is approximately twice that of $AgBi_3Se_5$. However, our results indicate that they have similar values. This could be due to the fact that the Boltzmann-Madsen theory takes into account group velocities and relaxation times, and does not consider the effective mass [8]. Despite this, due to the figure of merit for $AgBi_3Se_5$, this material is considered promising for thermoelectric materials science.

Acknowledgements

We would like to thank financial support of CONAHCYT (Mx).

1. J. H. Grebenkemper *et al*., High temperature thermoelectric properties of $Yb_{14}MnSb_{11}$ prepared from reaction of MnSb with the elements, *Chemistry of Materials* **27** (2015) 5791, https://doi.org/10.1021/acs.chemmater.5b02446
2. A. Bugalia, V. Gupta, and N. Thakur, Strategies to enhance the performance of thermoelectric materials: a review, *Journal of Renewable and Sustainable Energy* **15** (2023) 032704, https://doi.org/10.1063/5.0147000.
3. S. R. Brown *et al*., $Yb_{14}MnSb_{11}$: New high efficiency thermoelectric material for power generation, *Chemistry of Materials* **18** (2006) 1873, https://doi.org/10.1021/cm060261t
4. J. Zhang *et al*., High-performance pseudocubic thermoelectric materials from non-cubic chalcopyrite compounds, *Advanced Materials* **26** (2014) 3848, https://doi.org/10.1002/adma.201400058
5. T. Feng and X. Ruan, Prediction of spectral phonon mean free path and thermal conductivity with applications to thermoelectrics and thermal management: a review, *Journal of Nanomaterials* **2014** (2014) 206370, https://doi.org/10.1155/2014/206370
6. Z. Tong *et al*., Comprehensive first-principles analysis of phonon thermal conductivity and electron-phonon coupling in different metals, *Phys. Rev. B* **100** (2019) 144306, https://journals.aps.org/prb/abstract/10.1103/PhysRevB.100.144306
7. W. Wang, D. Thesiya, and S. M. Mukhopadhyay, Hierarchical hybrid heat sink material for thermo-electric generators, *Appl. Therm. Eng.* **236** (2023) 121674, https://doi.org/10.1016/j.applthermaleng.2023.121674
8. G. K. H. Madsen, J. Carrete, and M. J. Verstraete, Boltz- TraP2, a program for interpolating band structures and calculating semi-classical transport coefficients, *Comput. Phys. Commun.* **231** (2018) 140, https://doi.org/10.1016/j.cpc.2018.05.010
9. H. J. Goldsmid, Improving the thermoelectric figure of merit, *Sci. Technol. Adv. Mat.* **22** (2021) 280, https://doi.org/10.1080/14686996.2021.1903816.
10. C. Sevik and T. Çağın, Ab initio study of thermoelectric transport properties of pure and doped quaternary compounds, *Phys. Rev. B* **82** (2010) 045202, https://doi.org/10.1103/PhysRevB.82.045202.
11. G. J. Snyder and E. S. Toberer, Complex thermoelectric materials, *Nature Materials* **7** (2008) 105, https://doi.org/10.1038/nmat2090
12. T. Deng *et al.*, High-Throughput Strategies in the Discovery of Thermoelectric Materials, *Adv. Mater.* **36** (2024) 2311278, https://doi.org/10.1002/adma.202311278.
13. S. Khan *et al.*, Electronic and thermoelectric properties of YbMg2X2 (X = P, As, Sb, Bi) Zintl compounds by firstprinciples method, *J. Rare Earths* **42** (2022) 147, https://doi.org/10.1016/j.jre.2022.11.018.
14. J.-H. Kim *et al.*, Crystal Growth, Thermoelectric Properties, and Electronic Structure of $AgBi_3S_5$ and $AgSb_xBi_{3-x}S_5$ ($x = 0.3$), *Chem. Mater.* **17** (2005) 3606, https://doi.org/10.1021/cm0502931
15. Z.-H. Ge *et al*., Fabrication and properties of $Bi_{2-x}Ag_{3x}S_3$ thermoelectric polycrystals, *J. Alloys Compd.* **514** (2012) 205, https://doi.org/10.1016/j.jallcom.2011.11.072
16. L.-J. Zhang *et al*., Synthesis and transport properties of AgBi3S5 ternary sulfide compound, *Intermetallics* **36** (2013) 96, https://doi.org/10.1016/j.intermet.2013.01.013
17. G. Tan *et al*., High Thermoelectric Performance in Electron-Doped AgBi3S5 with Ultralow Thermal Conductivity, *J. Am. Chem. Soc.* **139** (2017) 6467, https://doi.org/10.1021/jacs.7b02399
18. Y. Wu *et al*., Boosting Thermoelectric Properties of AgBi3 (Se yS(1-y) 5 Solid Solution via Entropy Engineering, *ACS Applied Materials & Interfaces* **13** (2021) 4185, https://doi.org/10.1021/acsami.0c19387
19. D. Guo *et al*., The anisotropic thermoelectricity property of AgBi3S5 by first-principles study, *Journal of Alloys and Compounds* **773** (2019) 812, https://doi.org/10.1016/j.jallcom.2018.09.336
20. P. Blaha *et al.*, WIEN2k, An Augmented Plane Wave + Local Orbitals Program for Calculating Crystal Properties (2001).
21. F. Tran and P. Blaha, Accurate band gaps of semiconductors and insulators with a semilocal exchange-correlation potential, *Physical Review Letters* **102** (2009) 226401, https://doi.org/10.1103/PhysRevLett.102.226401
22. W. Li *et al*., ShengBTE: A solver of the Boltzmann transport equation for phonons, *Computer Physics Communications* **185** (2014) 1747, https://doi.org/10.1016/j.cpc.2014.02.015
23. S. Kirklin *et al.*, The Open Quantum Materials Database (OQMD): assessing the accuracy of DFT formation energies, *npj Computational Materials* **1** (2015) 15010, https://doi.org/10.1038/npjcompumats.2015.10
24. J. P. Perdew, K. Burke, and M. Ernzerhof, Generalized Gradient Approximation Made Simple, *Physical Review Letters* **77** (1996) 3865, https://doi.org/10.1103/PhysRevLett.77.3865
25. T. Scheidemantel *et al*., Transport coefficients from firstprinciples calculations, *Phys. Rev. B* **68** (2003) 125210, https://doi.org/10.1103/PhysRevB.68.125210
26. P. Sun *et al*., Large Seebeck effect by charge-mobility engineering, *Nature communications* **6** (2015) 7475, https://doi.org/10.1038/ncomms8475
27. B. Xu and M. J. Verstraete, First principles explanation of the positive Seebeck coefficient of lithium, *Physical Review Letters* **112** (2014) 196603, https://doi.org/10.1103/PhysRevLett.112.196603
28. D. Behera *et al*., Structural, electronic, optical, and thermoelectric response of Zintl phase AAg2S2 (A = Sr/Ba) compounds for renewable energy applications, *Physica B: Condensed Matter* **649** (2023) 414446, https://doi.org/10.1016/j.physb.2022.414446
29. J. Shuai, Layer-Structured Zintl Phases as Novel Thermoelectric Materials (2023), https://uh-ir.tdl.org/items/5232f8d4-b9f9-4bbc-9c67-61eba8111cde.